

On the Validity of Isotropic Complex α -Stable Interference Models for Interference in the IoT

Ce ZHENG¹, Malcolm EGAN², Laurent CLAVIER¹, Gareth W. PETERS³, Jean-Marie GORCE²

¹IMT Lille Douai, Univ. Lille, IEMN CNRS UMR 8520
50 Avenue Halley, 59650 Villeneuve-d'Ascq, France

²Université de Lyon, INSA Lyon, INRIA, CITI Lab
6 Avenue des Arts, 69621 Villeurbanne, France

³School of Mathematical and Computer Sciences, Heriot-Watt University
Edinburgh, Currie EH14 4AL, UK

ce.zheng.etu@univ-lille.fr, malcom.egan@insa-lyon.fr
laurent.clavier@telecom-lille.fr, g.peters@hw.ac.uk, jean-marie.gorce@insa-lyon.fr

Résumé – La croissance incessante d’objets communicants contraint les industriels et les chercheurs à développer des solutions permettant aux communications de rester fiables dans des environnements où l’interférence n’est pas Gaussienne. Un modèle précis de cette interférence est avant tout nécessaire et plusieurs propositions ont été faites comme le modèle de Middleton ou les distributions α -stables. Cet article étudie cette dernière proposition qui repose *a priori* sur des hypothèses peu réalistes, en particulier une puissance reçue non bornée. Nous montrons que ce modèle s’avère cependant valide, même si l’on introduit une zone de garde autour du récepteur, limitant la puissance à une valeur finie, en adaptant l’exposant caractéristique de la distribution. Ceci est validé par l’étude des quantiles. La structure de dépendance est également étudiée.

Abstract – With the growing numbers of IoT devices, both industries and researchers are facing the challenge of handling interference with non-Gaussian behavior. To model such interference, theoretical approaches have been proposed such as Middleton Class A and B, α -stable, etc. This paper addresses the validity of the α -stable model. Its theoretical validity is based on idealistic assumptions, especially an unbounded received power. We show that the α -stable model remains accurate, if we adapt the characteristic exponent α , when we introduce a guard zone that limits the received power. To do so, we study three features: the characteristic exponent, the quantiles and the dependence structure.

1 Introduction

Impulsiveness is a significant feature of the interference in the wireless network for Internet of Things (IoT). With large deployments of transmitting devices, even if they operate at low power levels, the amplitude of interference is more likely to be large compared with standard Gaussian models. Such a behavior has been observed both in recent experimental studies [1] and also in theoretical analysis [2]. As a consequence, Gaussian models are often not appropriate and the interference statistics lie in a more general class of models.

To model the impulsive nature of the interference, the Middleton Class A model has been widely adopted. Such interference arises when devices are located according to a homogeneous Poisson point process (PPP) with the guard bands, finite network radius, independent fading and baseband emissions. However, the Middleton model has a complicated representation, both in the form of its probability density function (PDF) and its characteristic function (CF). It also only forms an approximation of the interference in more realistic point process models, such as the Poisson-Poisson cluster process studied in [3].

A more tractable alternative is the complex α -stable interference model. This model can be viewed as the limiting case of the Middleton model when the guard band and network radii tend to zero and infinity, respectively. Although it is more difficult to work with than Gaussian models, it captures the heavy-tailed nature of the interference observed experimentally. However, an open question is, quantitatively, how well the α -stable model approximates more realistic network models.

In this paper, we focus on the validity of the α -stable interference assumption. Our study is based on a comparison of the α -stable model with interference simulated in a network of finite radius interferers and the presence guard-zones. We study three features of the interference models: the estimated characteristic exponent $\hat{\alpha}$; the quantiles of the interference distributions, i.e., Q-Q plots; and the dependence structure (a precise description is provided in Section 4). We find for realistic device densities that when the guard-zone radii do not exceed 5 metres, the α -stable model with theoretical characteristic exponent $\alpha = \frac{4}{\eta}$ where η is the path-loss exponent, is a good approximation. And the estimated stable model with $\hat{\alpha}$ keeps as a good approximation for different choices of guard zone radii.

2 System Model

Consider a network of devices located according to a homogeneous (PPP) with intensity λ , denoted by Φ . These devices form interferers for a receiver located at the origin. While such a model has been widely studied and will play an important role in this paper, practical considerations require that there is a minimum distance between the receiver and the closest interferer, r_{\min} or the expected received power from each interfering device does not exceed a maximum value.

To account for the effect of non-zero guard zone radii, the interference at the origin for a given time slot is given by

$$Z = \sum_{j \in \Phi} a(r_j) h_j x_j \quad (1)$$

where r_j is the distance from device j to the origin, η is the path loss exponent, $h_j \sim \mathcal{CN}(0, 1)$ is a Rayleigh fading coefficient, and x_j is the baseband emission. To capture the effect of guard zones, the signal attenuation is governed by

$$a(r) = \begin{cases} r^{-\eta/2}, & r \geq r_{\min} \\ 0, & r < r_{\min}. \end{cases} \quad (2)$$

A statistical characterization based on the characteristic function of the interference Z have been obtained by Gulati [3] and Sousa [4]. However, the resulting models are not analytically tractable. To this end, we study the isotropic α -stable model, which is known to be the exact distribution of Z when the guard zone radius $r_{\min} \rightarrow 0$ [2, 5, 6]. In the following section, we recall the definitions and key properties for the class of isotropic α -stable random variables.

3 Isotropic α -Stable Random Variables

The α -stable random variables have heavy-tailed PDF, which have been widely used to model impulsive signals [7]. The distribution of an α -stable random variable is parameterized by four parameters : the characteristic exponent $0 < \alpha \leq 2$; the scale parameter $\gamma \in \mathbb{R}_+$; the skew parameter $\beta \in [-1, 1]$; and the shift parameter $\delta \in \mathbb{R}$. As such, a common notation for an α -stable random variable X is $X \sim S_\alpha(\gamma, \beta, \delta)$.

In general, α -stable random variables do not have closed-form PDFs. Instead, they are usually represented by their characteristic function, given by [7, Eq. 1.1.6]

$$\mathbb{E}[e^{i\theta X}] = \begin{cases} \exp\{-\gamma^\alpha |\theta|^\alpha (1 - i\beta(\text{sign}\theta) \tan \frac{\pi\alpha}{2}) + i\delta\theta\}, & \alpha \neq 1 \\ \exp\{-\gamma |\theta| (1 + i\beta \frac{2}{\pi}(\text{sign}\theta) \log |\theta|) + i\delta\theta\}, & \alpha = 1 \end{cases} \quad (3)$$

In the case $\beta = \delta = 0$, X is said to be a symmetric α -stable random variable, denoted as $S_{\alpha S}$.

Isotropic complex α -stable random variables can now be defined as follows [7, Definition 2.6.2] :

Definition 1. Let Z_1, Z_2 be two symmetric α -stable random variables. The complex α -stable random variable $Z = Z_1 + iZ_2$ is isotropic if it satisfies the condition

$$e^{i\phi} Z \stackrel{(d)}{=} Z \text{ for any } \phi \in [0, 2\pi). \quad (4)$$

A complex α -stable random variable Z in (4) can be expressed as a vector $\mathbf{Z} = [Z_1, Z_2]$. A particular class of α -stable random vectors is an instance of the sub-Gaussian α -stable random vectors¹, defined as follows.

Definition 2. Any vector distributed as $\mathbf{X} = \sqrt{A}(G_1, \dots, G_d)$, where

$$A \sim S_{\alpha/2}((\cos \pi\alpha/4)^{2/\alpha}, 1, 0), \quad (5)$$

and $\mathbf{G} = [G_1, \dots, G_d] \sim \mathcal{N}(\mathbf{0}, \sigma^2 \mathbf{I})$ is called a sub-Gaussian $S_{\alpha S}$ random vector with underlying Gaussian vector \mathbf{G} .

The following proposition [7, Corollary 2.6.4] highlights the link between isotropic α -stable random variables and sub-Gaussian α -stable random vectors.

Proposition 1. Let $0 < \alpha < 2$. A complex α -stable random variable $Z = Z_1 + iZ_2$ is isotropic if and only if there are two independent and identically distributed zero-mean Gaussian random variables G_1, G_2 with variance σ^2 and a random variable $A \sim S_{\alpha/2}((\cos(\pi\alpha/4))^{2/\alpha}, 1, 0)$ independent of $(G_1, G_2)^T$ such that $(Z_1, Z_2)^T = A^{1/2}(G_1, G_2)^T$. That is, $(Z_1, Z_2)^T$ is a sub-Gaussian $S_{\alpha S}$ random vector.

4 α -Stable Interference Approximation

The key question that we address in this paper is under which conditions is the isotropic α -stable model a good approximation of the interference arising in the system model detailed in Section 2. To address this question, we proceed numerically by studying the quantiles of the marginals and the dependence between the real and imaginary parts via copula. In particular, we generate a simulated data set based on the system model in Section 2 and compare it with the theoretical and fitted isotropic α -stable model. In the numerical results, the intensity $\lambda = 0.001 \text{ m}^{-2}$ and the pathloss $\eta = 5$, which corresponds to an average of one device in a disc of radius of approximately 18 m and a non-line of sight pathloss environment (e.g., indoor or urban).

4.1 Properties of the Marginal Distributions

We first examine the distributions of real and imaginary parts of the interference in Section 2. In the isotropic α -stable model, the real and imaginary parts are $S_{\alpha S}$ random variables.

It has been shown that the marginal distribution is α -stable with $\alpha = \frac{4}{\eta}$ when $r_{\min} \rightarrow 0$ [6]. Hence, to obtain further insights into the impact of the guard zone radius r_{\min} on the behavior of the distributions, we first study Q-Q plots of the real or imaginary parts of the interference Z . In particular, we plot the quantiles for the interference estimated from the simulated data set with $r_{\min} > 0$, denoted by Q_I , against the quantiles for the theoretical model with $r_{\min} = 0$, denoted by Q_0 . Note that

1. There exist also sub-Gaussian stable vectors allowing for more general dependence structure [7], but are not necessary for the purposes of this paper.

when the two distributions are the same, the Q-Q plot exhibits a straight line.

Fig. 1 shows the Q-Q plots for varying r_{\min} . When $r_{\min} \leq 5$ m, the theoretical model is in good agreement with the simulated data. In particular, the figures exhibit straight lines. For $r_{\min} > 5$ m, the quantiles begin to significantly differ, implying that $\alpha = \frac{4}{\eta}$ is not a good approximation. Hence, we fit the data set to the stable model to get the estimated characteristic exponent $\hat{\alpha}$.

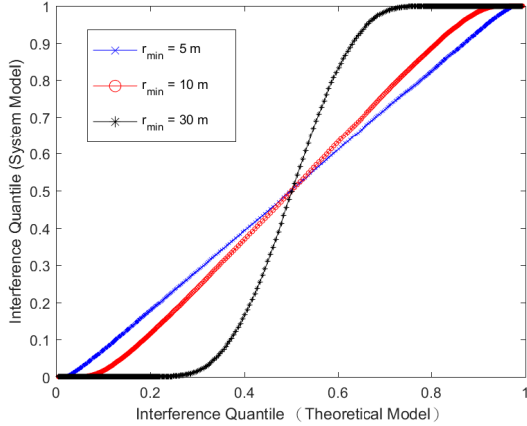


FIGURE 1 – Q-Q plots, the system model ($r_{\min} > 0$) against the theoretical model ($r_{\min} = 0$)

Fig. 2 shows the effect of increasing the guard zone radius r_{\min} . Observe that for small r_{\min} , $\hat{\alpha}$ is approximately 0.8, as expected from the theoretical model. On the other hand, as r_{\min} goes beyond 5 m, $\hat{\alpha}$ increases from 0.9 to approximately 2 for $r_{\min} > 30$ m. This implies that for very large choices of r_{\min} , a Gaussian model is the best fit. Nevertheless, for $r_{\min} < 30$ m, the Gaussian model is not a good choice.

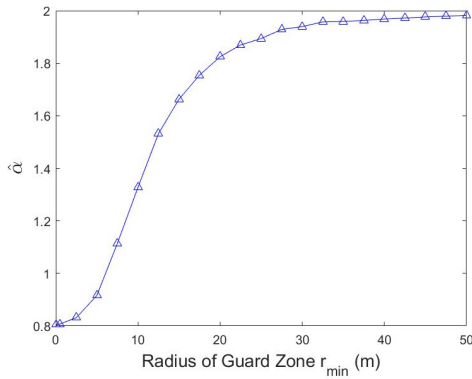


FIGURE 2 – Estimated $\hat{\alpha}$ under different guard zone radii

Furthermore, we keep Q_I and replace Q_0 with the quantiles for the fitted stable model with $\hat{\alpha}$ in Fig. 3. In Fig. 3, when $r_{\min} \leq 5$ m, the estimated model is in good agreement with the simulated data, which is consistent with Fig. 1 due to $\hat{\alpha} \approx$

0.8 as shown in Fig. 2. For $r_{\min} > 5$ m, the quantiles start to slightly differ, but still remains approximately as a straight line. However, when $r_{\min} > 30$ m, the Q-Q plot is approximately a straight line again for the reason that $\hat{\alpha}$ is close to 2 as shown in Fig. 2, indicating a more Gaussian behavior. This validates that the estimated stable model keeps a good approximation for different r_{\min} .

4.2 Dependence Structure

It is first important to mention that the isotropic α -stable random vector contains some dependency between the different dimensions as long as $\alpha < 2$, while the isotropic Gaussian vector results in uncorrelated dimensions. As such, it is useful to have tractable representations of the joint probability density function.

A popular method in statistics for tractably modeling non-Gaussian multivariate distributions is based on copulas. In the copula modeling approach, the joint distribution function of a random vector in \mathbb{R}^n , say $\mathbf{X} = [X_1, \dots, X_n]^T$, is given as

$$F(x_1, \dots, x_n) = C(F_1(x_1), \dots, F_n(x_n)), \quad (6)$$

where $C : [0, 1]^n \rightarrow [0, 1]$ is called a *copula function*, and F_i , $i = 1, \dots, n$ are the marginal distribution functions.

The copula of a multivariate distribution can be viewed as capturing the dependence structure of the distribution. Moreover, this dependence structure can be investigated by transforming a random vector \mathbf{X} in \mathbb{R}^n to the *copula space* via the transformation $(x_1, \dots, x_n) \mapsto (F_1(x_1), \dots, F_n(x_n))$. This perspective is useful as it reveals non-linear dependencies in data, which are often more important than linear dependencies in the case of heavy-tailed data (e.g., in α -stable models ($\alpha < 2$), covariances are infinite) [8, 9].

Fig. 4 shows the scatter plots for the simulated data set corresponding to different r_{\min} . Observe that in Fig. 4e, the scatter plot is approximately uniform, which implies that the real and imaginary parts of the interference are independent. This is expected because the interference Z is isotropic and in the regime $r_{\min} > 30$ m approximately Gaussian. In particular, if a complex Gaussian random variable is isotropic, then it is well known that its real and imaginary parts are independent.

On the other hand, when $r_{\min} < 5$ m the scatter points are concentrated in a non-uniform manner. In this regime, we have already seen that the distributions for the real and imaginary parts of the interference are approximately symmetric α -stable. For $\alpha < 2$, isotropic complex α -stable random variables do not have independent real and imaginary parts. This is particularly evident by the concentration of points in the corners of the scatter plot. The consequence is that when the magnitude of the real part of the interference is large, there is a greater probability of the imaginary part of the interference to have a large magnitude than in the Gaussian model.

Fig. 4c and Fig. 4d show the impact of further increasing r_{\min} . In these cases, the scatter plot is again non-uniform, which means that the Gaussian model is not an appropriate choice.

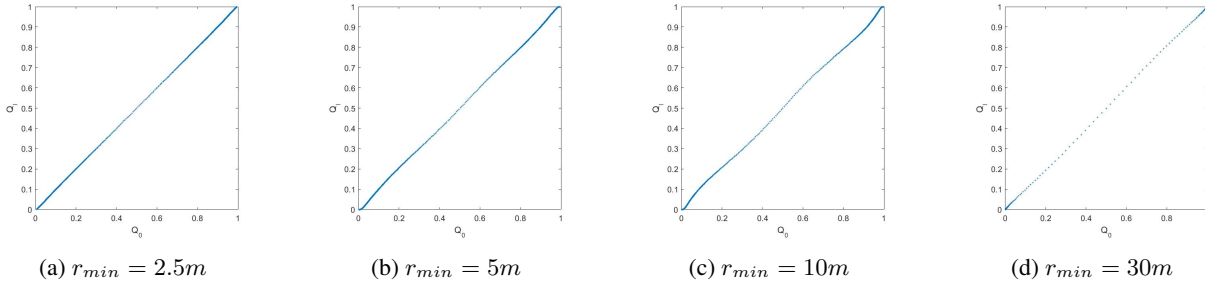


FIGURE 3 – Q-Q plots, the system model ($r_{min} > 0$) against the fitted model ($\hat{\alpha}$)

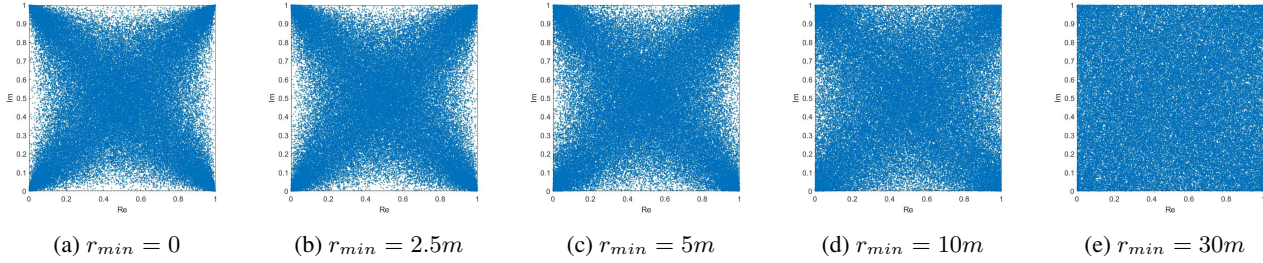


FIGURE 4 – Samples in Copula space under different r_{min}

5 Conclusions

Interference modeling for the IoT is challenging due to the fact that the interference is often impulsive, ruling out Gaussian models. While there has been significant work investigating good approximations for the interference distribution, an extensive investigation into the impact of practical network parameters has not been carried out. In this work, we have studied when an isotropic α -stable model forms a good approximation for the interference distribution. This study investigated both the impact of non-zero guard zone radii on the marginal distributions and the joint distribution. For realistic network parameters, isotropic α -stable models are a significantly better choice than Gaussian models.

Acknowledgements

This work has been (partly) funded by the French National Agency for Research (ANR) under grant ANR-16-CE25-0001 - ARBURST.

Fruitful discussions in the framework of the COST ACTION CA15104, IRACON and in IRCICA, USR CNRS 3380 have also contributed to this work.

Références

- [1] B. Vejlggaard, M. Lauridsen, H. Nguyen, I. Kovács, P. Mogensen, and M. Sørensen, “Interference impact on coverage and capacity for low power wide area IoT networks,” in *IEEE Wireless Communications and Networking Conference (WCNC)*, 2017.
- [2] M. Egan, L. Clavier, M. de Freitas, L. Dorville, J.-M. Gorce, and A. Savard, “Wireless communication in dynamic interference,” in *IEEE Global Communications Conference (GLOBECOM)*, 2017.
- [3] K. Gulati, B. Evans, J. Andrews, and K. Tinsley, “Statistics of co-channel interference in a field of Poisson-Poisson clustered interferers,” *IEEE Transactions on Signal Processing*, vol. 58, no. 12, pp. 6207–6222, 2010.
- [4] E. S. Sousa, “Performance of a spread spectrum packet radio network link in a poisson field of interferers,” *IEEE Transactions on Information Theory*, vol. 38, no. 6, pp. 1743–1754, 1992.
- [5] M. Egan, M. de Freitas, L. Clavier, A. Goupil, G. Peters, and N. Azzaoui, “Achievable rates for additive isotropic alpha-stable noise channels,” in *Proc. of the IEEE International Symposium on Information Theory*, 2016.
- [6] M. Egan, L. Clavier, C. Zheng, M. de Freitas, and J.-M. Gorce, “Dynamic interference for uplink SCMA in large-scale wireless networks without coordination,” *EURASIP Journal on Wireless Communications and Networking*, vol. 1, 2018.
- [7] G. Samorodnitsky and M. Taqqu, *Stable Non-Gaussian Random Processes*. New York, NY : CRC Press, 1994.
- [8] X. Yan, L. Clavier, G. Peters, N. Azzaoui, F. Septier, and I. Nevat, “Skew-t copula for dependence modelling of impulsive (alpha-stable) interference,” in *IEEE International Conference on Communications (ICC)*, 2015.
- [9] C. Zheng, M. Egan, L. Clavier, G. Peters, and J.-M. Gorce, “Copula-based interference models for IoT wireless networks,” in *Proc. IEEE International Conference on Communications (ICC)*, 2019.